Vibrational Energy Relaxation in Liquid Oxygen from a Semiclassical Molecular Dynamics Simulation

ARTICLE *in* THE JOURNAL OF PHYSICAL CHEMISTRY A · OCTOBER 2003

Impact Factor: 2.69 · DOI: 10.1021/jp0304982

2 AUTHORS, INCLUDING:

Qiang Shi
Chinese Academy of Sciences
101 PUBLICATIONS **2,414** CITATIONS

Vibrational Energy Relaxation in Liquid Oxygen from a Semiclassical Molecular Dynamics Simulation

Qiang Shi and Eitan Geva*

Department of Chemistry, University of Michigan, Ann Arbor, Michigan 48109-1055

Received: April 24, 2003; In Final Form: August 6, 2003

The semiclassical theory of vibrational energy relaxation (VER) developed in the preceding paper is extended to the case of molecular liquids, and used for calculating the VER rate constant in neat liquid oxygen at 77 K. We employ a semiclassical approximation of the quantum-mechanical force-force correlation function (FFCF), which puts it in terms of the Wigner transforms of the force and the product of the Boltzmann operator and the force. The multidimensional Wigner integrals are performed via a novel implementation of the local harmonic approximation (LHA). The methodology is extended to include centrifugal forces, and effective ways are developed in order to make it applicable to molecular liquids. The fact that VER of high-frequency solutes is dominated by the solvent molecules in their close vicinity suggests that the semiclassical treatment is restricted to the small cluster of molecules around the relaxing molecule. The rest of the molecules are frozen and serve as a static cage that keeps the cluster from falling apart. The method is applied to the challenging problem of calculating the extremely slow ($k_{0\leftarrow 1} = 395\ s^{-1}$) and highly quantum-mechanical ($\hbar\omega/k_BT = 29$) VER rate constant in neat liquid oxygen at 77 K. The results are found to be in very good quantitative agreement with experiment and suggest that this semiclassical approximation can capture the 4 orders of magnitude quantum enhancement of the experimentally observed VER rate constant over the corresponding classical prediction. As for the simpler models considered in the preceding paper, we find that VER in liquid oxygen is dominated by a purely quantum mechanical term, which vanishes at the classical limit. These results further establish the semiclassical method as an attractive alternative to the commonly used approach which is based on ad hoc quantum correction factors.

I. Introduction

The problem of vibrational energy relaxation (VER) in liquid solutions has received much attention over the last few decades.[1−39] The VER rate provides a sensitive probe of intramolecular dynamics and solute−solvent interactions, which are known to have a crucial impact on other important properties, such as chemical reactivity, solvation dynamics, and transport coefficients. The simulation of VER in liquid solutions has presented theoretical chemistry with an ongoing challenge due to the high frequency of most molecular vibrations (in the sense that $\hbar\omega/k_BT \gg 1$). One implication of the high frequency is that VER is often found to be slow, due to the low density of accepting modes with matching frequencies, and therefore cannot be obtained directly from nonequilibrium MD simulations. This problem is usually circumvented by resorting to the Landau−Teller (LT) formula, which gives the VER rate constant in terms of the Fourier transform (FT), at the vibrational frequency, of a certain short-lived force-force correlation function (FFCF), which can be calculated from equilibrium MD simulations with a rigid solute. Another difficulty has to do with the fact that extracting the very small high-frequency Fourier components of the FFCF can become extremely difficult due to statistical noise accompanying all real-life simulations. This difficulty is often dealt with by using an extrapolation of the exponential gap law, which usually emerges at low frequencies, to much higher frequencies.[40,41] An alternative, yet similar, approach combines a short time expansion of the FFCF with a parametrized ansatz that exhibits an exponential gap law behavior at high frequencies, whose FT can be calculated analytically.[42−50]

Another fundamental difficulty imposed by the fact that $\hbar\omega/k_BT \gg 1$, is that the *quantum-mechanical* FFCF, rather than the *classical* FFCF, should be used in the LT formula. The exact calculation of real-time quantum-mechanical correlation functions for general many-body systems remains far beyond the reach of currently available computer resources, due to the exponential scaling of the computational effort with the number of degrees of freedom (DOF).[51] The most popular approach for dealing with this difficulty is to first evaluate the FT of the classical FFCF, and then multiply the result by a frequency-dependent *quantum correction factor* (QCF).[1,52−67] Various approximate QCFs have been proposed in the literature. Unfortunately, estimates obtained from different QCFs can differ by orders of magnitude, and particularly so when high-frequency vibrations are involved.

In the preceding paper,[124] which will be referred to below as paper I, we developed a new method for calculating the quantum-mechanical FFCF which is based on the linearized-semiclassical initial-value-representation (LSC−IVR) approximation. The LSC−IVR approximation has been recently derived by Miller and co-workers[68−74] via linearizing the forward−backward action in the semiclassical[51,68,69,74−99] initial value representation[86−89,98,100−107] expression for a real-time quantum-mechanical correlation function, with respect to the difference between the forward and backward trajectories. We have recently shown that the very same approximation can also be

* Corresponding author. E-mail: eitan@umich.edu.

10.1021/jp0304982 CCC: $25.00
Published on Web 10/04/2003

derived by linearizing the *exact* real-time path integral expression for the correlation function, without explicitly invoking the semiclassical approximation.[108]

The LSC−IVR approximation for a general real-time correlation function is given by [here, as in the rest of this paper, we use boldface symbols for vectors, and capped symbols (e.g. $\hat{A}$) for operators]:

$$\mathrm{Tr}(e^{-\beta\hat{H}}e^{i\hat{H}t/\hbar}\hat{B}e^{-i\hat{H}t/\hbar}\hat{A}) \approx \frac{1}{(2\pi\hbar)^f}\int \mathbf{dq_0}\int \mathbf{dp_0}(\hat{A}e^{-\beta\hat{H}})_W(\boldsymbol{q_0},\boldsymbol{p_0})B_W(\boldsymbol{q_t}^{(Cl)},\boldsymbol{p_t}^{(Cl)}), \quad (1)$$

where, f is the number of DOF, $\boldsymbol{q_0} = (q_0^{(1)}, ..., q_0^{(f)})$ and $\boldsymbol{p_0} = (p_0^{(1)}, ..., p_0^{(f)})$ are the corresponding coordinates and momenta

$$A_W(\boldsymbol{q_0},\boldsymbol{p_0}) = \int \mathbf{d}\Delta\, e^{-i\boldsymbol{p}_0\Delta/\hbar}\langle \boldsymbol{q}_0 + \Delta/2|\,\hat{A}\,|\boldsymbol{q}_0 - \Delta/2\rangle \quad (2)$$

is the Wigner transform of $\hat{A}$,[109] and $\boldsymbol{q_t}^{(Cl)} = \boldsymbol{q_t}^{(Cl)}(\boldsymbol{q_0},\boldsymbol{p_0})$ and $\boldsymbol{p_t}^{(Cl)} = \boldsymbol{p_t}^{(Cl)}(\boldsymbol{q_0},\boldsymbol{p_0})$ are propagated classically with the initial conditions $\boldsymbol{q_0}$ and $\boldsymbol{p_0}$. The major advantage of LSC−IVR has to do with its computational feasibility (although computing the Wigner transform in systems with many DOF is not trivial[69]). The LSC−IVR approximation has the additional attractive features of being exact at $t = 0$, at the classical limit, and for harmonic systems. Its main disadvantage has to do with the fact that it can only capture quantum dynamical effects that arise from short-time interferences between the various trajectories (the longer time dynamics is purely classical).[70] However, it should be noted that generally in condensed phase, and particularly in the case of high-frequency VER, the quantities of interest are often dominated by the short-time dynamics of the correlation functions.

The major difficulty involved in using eq 1 for calculating the FFCF has to do with that fact that the calculation of the multidimensional Wigner phase-space integral, via conventional Monte Carlo (MC) techniques, is made extremely difficult by the oscillatory phase factor, $e^{-i\mathbf{P}_0\Delta/\hbar}$, in the integrand of eq 2. This problem was dealt with in paper I by using a novel implementation of the local harmonic approximation (LHA), which allowed for an analytical evaluation of the Wigner integral. The emerging method, which was designated LHA−LSC−IVR, has been tested in paper I on several model systems: (1) a vibrational mode coupled to a harmonic bath, with the coupling exponential in the bath coordinates; (2) a diatomic molecule coupled to a short chain of helium atoms that interact via Lennard-Jones (LJ) pair potentials; (3) A spherically symmetric diatomic molecule (a "breathing sphere"), in a two-dimensional monatomic LJ liquid. Very good agreement with the exact results, or their best estimates, has been found in all cases. It was also found in all cases that the quantum enhancement of the VER rate constant is dominated by a purely quantum mechanical term which is not accounted for in classical MD simulations.

In the present paper, we report on the first application of the LHA−LSC−IVR method to a truly molecular liquid in 3D. The more demanding nature of this problem required that the method is extended to cases involving centrifugal forces, as well as the development of effective ways for dealing with constrained systems and thousands of DOF. The resulting modified and extended LHA−LSC−IVR method is specialized for calculating the extremely slow ($k_{0\leftarrow1} = 395\ s^{-1}$) and highly quantum-mechanical ($\hbar\omega/k_BT = 29$) VER rate constant in neat liquid oxygen at 77 K. It should be noted that calculation of the VER rate constant in neat liquid oxygen, which has been measured some time ago at temperatures between 60K to 90K and under atmospheric pressure,[15] has proved to be extremely challenging in the past. A prediction based on purely classical MD simulations has been found to be smaller by 4 orders of magnitude relative to the corresponding experimental value, and no unique prediction can be obtained based on the QCF approach (see Table 1).[43,59]

TABLE 1: $k_{0\leftarrow1}$ for Near-Liquid O_2 at 77 K[a]

	$k_{0\leftarrow1}(s^{-1})$
classical	0.031 ± 0.0045
harmonic	5.2 ± 0.3
Egelstaff	1900 ± 300
mixed harmonic−Egelstaff	1000 ± 180
LHA−LSC−IVR	1600 ± 280
experiment	395

[a] The error in the LSC−IVR result is based on an estimated 15% error in the extrapolation.

The structure of the remainder of this paper is as follows. The model Hamiltonian of liquid oxygen and basic VER theory are outlined in section 2. The semiclassical theory of VER is described in section 3. The simulation techniques used for calculating the FFCF are described in section 4. The results for neat liquid oxygen at 77 K are reported and analyzed in section 5. We conclude in section 6 with a summary of the main results and some discussion on their significance.

II. Model and Formalism

Following Everitt et al. in ref 59, we consider a single vibrating oxygen molecule solute in a solvent that consists of N_m rigid oxygen molecules. The overall Hamiltonian is

$$\hat{H} = \hat{H}_q + \hat{T}(\hat{q}) + \hat{U}(\hat{q}) \quad (3)$$

where

$$\hat{H}_q = \frac{\hat{p}^2}{2\mu} + \frac{1}{2}\mu\omega_0{}^2\hat{q}^2, \quad (4)$$

$$T(q) = \frac{(\hat{P}_{CM}^{(0)})^2}{2M_m} + \frac{(\hat{L}^{(0)})^2}{2I^{(0)}(\hat{q})} + \sum_{i=1}^{N_m}\left(\frac{(\hat{P}_{CM}^{(i)})^2}{2M_m} + \frac{(\hat{L}^{(i)})^2}{2I}\right) \quad (5)$$

and

$$\hat{U}(\hat{q}) = \sum_{i=1}^{N_m}\sum_{j<i}\sum_{\alpha,\beta}\phi[|\hat{\boldsymbol{r}}^{(i\alpha)} - \hat{\boldsymbol{r}}^{(j\beta)}|] + \sum_{i=1}^{N_m}\sum_{\alpha,\beta}\phi[|\hat{\boldsymbol{r}}^{(i\alpha)} - \hat{\boldsymbol{r}}^{(0\beta)} - q\hat{\boldsymbol{u}}^{(0\beta)}/2|] \quad (6)$$

$\hat{T}(\hat{q})$ is the total rotational and translational kinetic energy, with M_m the *molecular* mass and $\hat{\boldsymbol{P}}_{CM}^{(0)}$, $\hat{\boldsymbol{L}}^{(0)}$ and $I^{(0)}(\hat{q}) = \mu(r_e + \hat{q})^2$ the center of mass momentum, angular momentum, and moment of inertia of the relaxing molecule, respectively. $\{\hat{\boldsymbol{P}}_{CM}^{(i)}\}$, $\{\hat{\boldsymbol{L}}^{(i)}\}$ and $I = \mu r_e{}^2$ are the center of mass momenta, angular momenta, and moment of inertia of the rest of the molecules, respectively. $\hat{U}(\hat{q})$ is the overall potential energy, which is given as a sum of site−site Lennard-Jones (LJ) pair potentials

$$\phi(r) = 4\epsilon\left[\left(\frac{\sigma}{r}\right)^{12} - \left(\frac{\sigma}{r}\right)^{6}\right] \quad (7)$$

with $\epsilon/k_B = 48.0$ K and $\sigma = 3.006$ Å.[59,110] Each O_2 molecule is described by two sites, one for each of the atoms, with an

equilibrium internuclear distance of 1.208 Å.[59,110] $\hat{\boldsymbol{r}}^{(i\alpha)}$ corresponds to the position of site α on the ith molecule, and $\hat{\boldsymbol{u}}^{(0\beta)}$ corresponds to a unit vector pointing from the center of mass of the relaxing molecule to its β site. The model used in ref 59 also included polarizable (q-dependent) σ and ϵ. However, the effect of this q-dependence on the resulting VER rate constant was found to be rather small. We therefore chose to neglect it in the treatment reported below.

The force is obtained by linearizing the Hamiltonian $T(q) + U(q)$ with respect to $\hat{q}$:

$$\hat{T}(\hat{q}) + \hat{U}(\hat{q}) \simeq \hat{T}(0) + \hat{U}(0) - \hat{q}\hat{F} \tag{8}$$

Here $\hat{F} = \hat{F}_T + \hat{F}_U$, with the *centrifugal force*,[111,112] $\hat{F}_T$, and *potential force*, $\hat{F}_U$,[113−115] given by

$$\hat{F}_T = -\left.\frac{\hat{T}(q)}{\partial q}\right|_{q=0} = \frac{(\hat{L}^{(0)})^2}{I^{(0)} r_e} \tag{9}$$

and

$$\hat{F}_U = -\left.\frac{\hat{U}(q)}{\partial q}\right|_{q=0} = \frac{1}{2}\sum_{i=1}^{N_m}\sum_{\alpha,\beta}\phi'(|\hat{\boldsymbol{r}}^{(i\alpha)} - \hat{\boldsymbol{r}}^{(0\beta)}|)\frac{(\hat{\boldsymbol{r}}^{(i\alpha)} - \hat{\boldsymbol{r}}^{(0\beta)})\cdot\hat{\boldsymbol{u}}^{(0\beta)}}{|\hat{\boldsymbol{r}}^{(i\alpha)} - \hat{\boldsymbol{r}}^{(0\beta)}|} \tag{10}$$

respectively. After the linearization, the overall Hamiltonian is given by

$$\hat{H} = \hat{H}_q + \hat{H}_b + \hat{H}_{bs} \tag{11}$$

where

$$\hat{H}_b = \hat{T}(0) + \hat{U}(0) = \sum_{i=0}^{N_m}\left(\frac{(\hat{P}_{CM}^{(i)})^2}{2M_m} + \frac{(\hat{L}^{(i)})^2}{2I}\right) + \sum_{i=0}^{N_m}\sum_{j<i}\sum_{\alpha,\beta}\phi(|\hat{\boldsymbol{r}}^{(i\alpha)} - \hat{\boldsymbol{r}}^{(0\beta)}|)\,, \tag{12}$$

and

$$\hat{H}_{bs} = -\hat{q}\hat{F} = -\hat{q}(\hat{F}_T + \hat{F}_U) \tag{13}$$

The experimentally measured[15] transition rate constant from the first excited vibrational state to the ground state of the relaxing O_2 molecule is given by the LT formula (cf. paper I):[9,116]

$$k_{0\leftarrow 1} = \frac{1}{2\mu\hbar\omega_0}\tilde{C}(\omega_0) \tag{14}$$

where

$$\tilde{C}(\omega_0) = \int_{-\infty}^{\infty} dt\, e^{i\omega_0 t} C(t), \tag{15}$$

and

$$C(t) = \langle\delta\hat{F}_0(t)\delta\hat{F}\rangle_0 = \frac{1}{Z_b}\mathrm{Tr}[e^{-\beta\hat{H}_b}e^{i\hat{H}_b t/\hbar}\delta\hat{F}e^{-i\hat{H}_b t/\hbar}\delta\hat{F}] \tag{16}$$

Here, $\langle\hat{A}\rangle_0 = \mathrm{Tr}[e^{-\beta\hat{H}_b}\hat{A}]/Z_b$, $Z_b = \mathrm{Tr}[e^{-\beta\hat{H}_b}]$, $\delta\hat{F} = \hat{F} - \langle\hat{F}\rangle_0$, and

$$\delta\hat{F}_0(t) = e^{i\hat{H}_b t/\hbar}\delta\hat{F}e^{-i\hat{H}_b t/\hbar} \tag{17}$$

Equation 14 gives the VER rate constant, $k_{0\leftarrow 1}$, in terms of the FT, at the vibrational frequency, ω_0, of the FFCF, $C(t)$.

It should be noted that although $C(t)$ is complex, i.e., $C(t) = C_R(t) + iC_I(t)$ with $C_R(t)$ and $C_I(t)$ the real and imaginary parts, respectively, its FT, $\tilde{C}(\omega)$, is real. Taking advantage of the general symmetries satisfied by $C(t)$, namely $C(-t) = C^*(t)$ and $\tilde{C}(-\omega) = e^{-\beta\hbar\omega}\tilde{C}(\omega)$, make it possible to compute $\tilde{C}(\omega)$ from either $C(t)$, $C_I(t)$, or $C_R(t)$:

$$\tilde{C}(\omega) = \frac{4}{1+e^{-\beta\hbar\omega}}\int_0^\infty dt\cos(\omega t)C_R(t) = -\frac{4}{1-e^{-\beta\hbar\omega}}\int_0^\infty dt\sin(\omega t)C_I(t) \tag{18}$$

III. A Semiclassical Formula for the VER Rate Constant

For the sake of developing the LSC−IVR approximation for the FFCF, eq 16, it is convenient to describe the system in terms of the *atomic* space-fixed Cartesian coordinates and adjoint momenta. To this end, let $\hat{\boldsymbol{Q}} = (\hat{Q}^{(1)}, ..., \hat{Q}^{(N)})$ and $\hat{\boldsymbol{P}} = (\hat{P}^{(1)}, ..., \hat{P}^{(N)})$ be the Cartesian coordinates and momenta of the *atoms*, with $N = 6(N_m + 1)$. We may therefore rewrite the bath Hamiltonian in eq 12 in the following way:

$$\hat{H}_b = \sum_{i=1}^{N}\frac{(\hat{P}^{(i)})^2}{2M} + \hat{V}(\hat{\boldsymbol{Q}}), \tag{19}$$

where $M = M_m/2$ is the atomic mass of oxygen, and $V(\hat{\boldsymbol{Q}}) = U(0)$. It should also be noted that the systems can only access nuclear configurations that satisfy the constraint of fixed interatomic distance in each diatom. Finally, we need to express the forces in eqs 9 and 10 in terms of the atomic coordinates and momenta. The potential force, F_U, is already given in terms of the atomic coordinates, through the site−site interaction terms [cf. eq 10]. The centrifugal force can be written in terms of the atomic momenta that correspond to the relaxing molecule:

$$\hat{F}_T = \frac{1}{2I^{(0)}}\{(\hat{P}_{\alpha,x}^{(0)} - \hat{P}_{\beta,x}^{(0)})^2 + (\hat{P}_{\alpha,y}^{(0)} - \hat{P}_{\beta,y}^{(0)})^2 + (\hat{P}_{\alpha,y}^{(0)} - \hat{P}_{\beta,y}^{(0)})^2\} \tag{20}$$

where, for example, $\hat{P}_{\alpha,x}^{(0)}$ is the x component of the momentum of the atom in the α site of the relaxing molecule.

The LSC−IVR approximation, eq 1, of the quantum-mechanical FFCF, eq 16, assumes the following form:

$$C(t) \approx \frac{1}{Z_b}\frac{1}{(2\pi\hbar)^N}\int d\boldsymbol{Q_0}\int d\boldsymbol{P_0}[\delta\hat{F}e^{-\beta\hat{H}_b}]_W(\boldsymbol{Q_0},\boldsymbol{P_0})\delta F_W(\boldsymbol{Q_t^{(Cl)}}, \boldsymbol{P_t^{(Cl)}}) \tag{21}$$

Here

$$\delta F_W(\boldsymbol{Q_t^{(Cl)}},\boldsymbol{P_t^{(Cl)}}) = \delta F_U(\boldsymbol{Q_t^{(Cl)}}) + \delta F_T(\boldsymbol{P_t^{(Cl)}}), \tag{22}$$

and

$$[\delta\hat{F}e^{-\beta\hat{H}_b}]_W(\boldsymbol{Q_0},\boldsymbol{P_0}) = \int \mathbf{d}\Delta e^{-i\mathbf{P}_0\Delta/\hbar}\langle\boldsymbol{Q_0} + \Delta/2|(\delta\hat{F}_T + \delta\hat{F}_U)e^{-\beta\hat{H}_b}|\boldsymbol{Q_0} - \Delta/2\rangle \tag{23}$$

A direct application of eq 21 to an anharmonic many-body system would require an exact numerical calculation of the

multidimensional Wigner phase-space integral in eq 23. Unfortunately, it is extremely difficult to perform this calculation via conventional Monte Carlo (MC) techniques, due to the oscillatory phase factor, $e^{-i\mathbf{P}_0\Delta/\hbar}$, in the integrand. One can overcome this obstacle by employing the LHA in order to perform the corresponding approximate Wigner integral analytically. The LHA has been applied to the potential force contribution to the Wigner integral of eq 23, $[\delta\hat{F}_U e^{-\beta\hat{H}_b}]_W$, in paper I, and the result obtained there can be immediately adopted for the application considered here (see below). However, the evaluation of the centrifugal force contribution, $[\delta\hat{F}_T e^{-\beta\hat{H}_b}]_W$, requires the extension of the LHA-based approach to momenta-dependent forces. Such an extension is presented below.

As in the case of the potential force, we start by introducing a quadratic expansion of the potential energy of the bath, $V(\boldsymbol{Q})$, around $\boldsymbol{Q_0}$, followed by a transformation of the bath Hamiltonian, $\hat{H}_b$, to the normal mode representation. This yields the following LHA of the quantum-mechanical bath Hamiltonian around $\boldsymbol{Q} = \boldsymbol{Q_0}$:

$$\hat{H}_b \approx \sum_{k=1}^{N} \frac{1}{2}(\hat{P}_n^{(k)})^2 + V(\boldsymbol{Q_0}) + \sum_{k=1}^{N} G_n^{(k)}\,\hat{Q}_n^{(k)} + \frac{1}{2}\sum_{k=1}^{N}(\Omega^{(k)})^2[\hat{Q}_n^{(k)}]^2 \quad (24)$$

where

$$Q_n^{(k)} = \sum_{l=1}^{N} T_{l,k}\sqrt{M}[Q^{(l)} - Q_0^{(l)}]\,,\ \hat{P}_n^{(k)}(\boldsymbol{Q_0}) = \sum_{l=1}^{N} T_{l,k}M^{-1/2}\hat{P}^{(l)} \quad (25)$$

are the mass-weighted normal mode coordinates and momenta, respectively, $\{(\Omega^{(k)})^2\}$ are the eigenvalues of the corresponding Hessian matrix, and

$$G_n^{(k)}(\boldsymbol{Q_0}) = \sum_{l=1}^{N} T_{l,k}M^{-1/2}\left.\frac{\partial V}{\partial Q^{(l)}}\right|_{\mathbf{Q}=\mathbf{Q}_0}. \quad (26)$$

We next rewrite the contribution of the centrifugal force to the Wigner transform in eq 23 in the following form:

$$[\delta\hat{F}_T e^{-\beta\hat{H}_b}]_W = \langle\boldsymbol{Q_0}|e^{-\beta\hat{H}_b}|\boldsymbol{Q_0}\rangle\int \boldsymbol{d}\Delta e^{-i\mathbf{P}_0\Delta/\hbar}\times \frac{\langle\boldsymbol{Q_0}+\Delta/2|\delta F_T(\hat{\boldsymbol{P}})e^{-\beta\hat{H}_b}|\boldsymbol{Q_0}-\Delta/2\rangle}{\langle\boldsymbol{Q_0}|e^{-\beta\hat{H}_b}|\boldsymbol{Q_0}\rangle} \quad (27)$$

We refrain from applying the LHA to the $\langle\boldsymbol{Q_0}|e^{-\beta\hat{H}_b}|\boldsymbol{Q_0}\rangle$ factor preceding the integral. However, we do apply the LHA of eq 24 in the evaluation of the ratio, $\langle\boldsymbol{Q_0}+\Delta/2|\delta F_T(\hat{\boldsymbol{P}})e^{-\beta\hat{H}_b}|\boldsymbol{Q_0}-\Delta/2\rangle/\langle\boldsymbol{Q_0}|e^{-\beta\hat{H}_b}|\boldsymbol{Q_0}\rangle$. To this end, we express $\hat{F}_T$ in eq 20 in terms of the normal mode momenta

$$\hat{F}_T = \sum_{k,l=1}^{N} C_{k,l}\hat{P}_n^{(k)}\,\hat{P}_n^{(l)}, \quad (28)$$

replace $\hat{H}_b$ by its LHA, eq 24, and use the following identities (the proportionality constants C_0, C_1, and C_2 are independent of Q_1 and Q_2)

$$\langle Q_1|e^{-\beta[\hat{P}^2/2+\Omega^2\hat{Q}^2/2]}|Q_2\rangle = C_0\exp\left\{-\frac{\Omega}{2\hbar}\frac{1}{\sinh(\beta\hbar\Omega)}\times [\cosh(\beta\hbar\Omega)(Q_1^{\,2}+Q_2^{\,2}) - 2Q_1Q_2]\right\},$$

$$\langle Q_1|\,\hat{P}e^{-\beta[\hat{P}2/2+\Omega2\hat{Q}^2/2]}|Q_2\rangle = iC_1\Omega\coth(\beta\hbar\Omega)\left(Q_1 - \frac{Q_2}{\cosh(\beta\hbar\Omega)}\right)\times \exp\left\{-\frac{\Omega}{2\hbar}\frac{1}{\sinh(\beta\hbar\Omega)}[\cosh(\beta\hbar\Omega)(Q_1^{\,2}+Q_2^{\,2}) - 2Q_1Q_2]\right\},$$

$$\langle Q_1|\,\hat{P}^2e^{-\beta[\hat{P}^2/2+\Omega2\hat{Q}^2/2]}|Q_2\rangle = C_2\left[\hbar\Omega\coth(\beta\hbar\Omega) - \omega^2\coth^2(\beta\hbar\Omega)\left(Q_1 - \frac{Q_2}{\cosh(\beta\hbar\Omega)}\right)^2\right] = \exp\left\{-\frac{\Omega}{2\hbar}\frac{1}{\sinh(\beta\hbar\Omega)}[\cosh(\beta\hbar\Omega)(Q_1^{\,2}+Q_2^{\,2}) - 2Q_1Q_2]\right\} \quad (29)$$

in order to explicitly evaluate $\langle\boldsymbol{Q_0}+\Delta/2|\delta F_T(\hat{\boldsymbol{P}})e^{-\beta\hat{H}_b}|\boldsymbol{Q_0}-\Delta/2\rangle/\langle\boldsymbol{Q_0}|\,e^{-\beta\hat{H}_b}|\boldsymbol{Q_0}\rangle$. This is followed by changing the integration variables from $\{\Delta^{(k)}\}$ to $\{\Delta_n^{(k)}\}$, where

$$\Delta_n^{(k)} = \sum_{k=1}^{N} T_{l,k}\sqrt{M^{(l)}}\,\Delta^{(l)} \quad (30)$$

and performing the Gaussian integrals over $\{\Delta_n^{(k)}\}$ analytically.

This procedure leads to the following result:

$$[\delta\hat{F}_T e^{-\beta\hat{H}_b}]_W = \langle\boldsymbol{Q_0}|e^{-\beta\hat{H}_b}|\boldsymbol{Q_0}\rangle\prod_{j=1}^{N}\left(\frac{4\pi}{M\alpha^{(j)}}\right)^{1/2}\exp\left[-\frac{(P_{n,0}^{(j)})^2}{\hbar^2\alpha^{(j)}}\right]\times \{\delta F_T(\boldsymbol{P_{n,0}}) + D_T(\boldsymbol{Q_0}, \boldsymbol{P_{n,0}})\} \quad (31)$$

where

$$\delta F_T(\boldsymbol{P_{n,0}}) = \sum_{k,l=1}^{N} C_{k,l}P_{n,0}^{(k)}\,P_{n,0}^{(l)}, \quad (32)$$

$$D_T(\boldsymbol{Q_0}, \boldsymbol{P_{n,0}}) = \sum_{k=1}^{N} C_{k,k}\frac{(\Omega^{(k)})^2}{2\alpha^{(k)}} + \frac{i}{\hbar}\sum_{k,l=1}^{N} C_{k,l}\left[\frac{G_n^{(k)}\,P_{n,0}^{(l)}}{\alpha^{(k)}} + \frac{G_n^{(l)}\,P_{n,0}^{(k)}}{\alpha^{(l)}}\right] - \frac{1}{\hbar^2}\sum_{k,l=1}^{N} C_{k,l}\frac{G_n^{(k)}\,G_n^{(l)}}{\alpha^{(k)}\alpha^{(l)}}, \quad (33)$$

and

$$\alpha^{(j)} = \frac{\Omega^{(j)}}{\hbar}\coth\,[\beta\hbar\Omega^{(j)}/2]. \quad (34)$$

The contribution of the potential force to the Wigner transform in eq 23, within the LHA, has been worked out in paper I and is given by

$$[\delta\hat{F}_U e^{-\beta\hat{H}_b}]_W = \langle\boldsymbol{Q_0}|e^{-\beta\hat{H}_b}|\boldsymbol{Q_0}\rangle\prod_{j=1}^{N}\left(\frac{4\pi}{M\alpha^{(j)}}\right)^{1/2}\exp\left[-\frac{(P_{n,0}^{(j)})^2}{\hbar^2\alpha^{(j)}}\right]\times [\delta F_U(\boldsymbol{Q_0}) + D_U(\boldsymbol{Q_0},\boldsymbol{P_{n,0}})], \quad (35)$$

where

$$D_U(\boldsymbol{Q_0},\boldsymbol{P_{n,0}}) = -i\sum_{k=1}^{N}\frac{(\tilde{F}'_U)_k P_{n,0}^{(k)}}{\hbar\alpha^{(k)}} + \sum_{k=1}^{N}\frac{(\tilde{F}''_U)_{k,k}}{4\alpha^{(k)}} - \sum_{k,l=1}^{N}\frac{(\tilde{F}''_U)_{k,l}P_{n,0}^{(k)}P_{n,0}^{(l)}}{2\hbar^2\alpha^{(k)}\alpha^{(l)}}, \quad (36)$$

$$(\tilde{F}'_U)_k = \sum_{l=1}^{N}(M^{(l)})^{-1/2}T_{l,k}(F'_U)_l;$$

$$(\tilde{F}''_U)_{k,l} = \sum_{i=1}^{N}\sum_{j=1}^{N}(M^{(i)}M^{(j)})^{-1/2}T_{i,l}T_{j,k}(F''_U)_{i,j}. \quad (37)$$

and

$$(F'_U)_k = \left.\frac{\partial F_U}{\partial Q^{(k)}}\right|_{\mathbf{Q}=\mathbf{Q}_0}; \quad (F''_U)_{k,l} = \left.\frac{\partial^2 F_U}{\partial Q^{(k)}\partial Q^{(l)}}\right|_{\mathbf{Q}=\mathbf{Q}_0}. \quad (38)$$

Substituting eqs 31 and 35 into eq 21 and changing the integration variables from $\{P_0^{(k)}\}$ to $\{P_{n,0}^{(k)}\}$ then lead to the final form of our approximate expression for the quantum-mechanical FFCF:

$$C(t) \approx \int d\boldsymbol{Q_0}\frac{\langle \boldsymbol{Q_0}|e^{-\beta\hat{H}_b}|\boldsymbol{Q_0}\rangle}{Z_b}\int d\boldsymbol{P_{n,0}}\prod_{j=1}^{N}\left(\frac{1}{\alpha^{(j)}\pi\hbar^2}\right)^{1/2} \times \exp\left[-\frac{(P_{n,0}^{(j)})^2}{\hbar^2\alpha^{(j)}}\right][\delta F_U(\boldsymbol{Q_0}) + \delta F_T(\boldsymbol{P_{n,0}}) + D_U(\boldsymbol{Q_0},\boldsymbol{P_{n,0}}) + D_T(\boldsymbol{Q_0},\boldsymbol{P_{n,0}})][\delta F_U(\boldsymbol{Q_t^{(Cl)}}) + \delta F_T(\boldsymbol{P_{n,t}^{(Cl)}})]. \quad (39)$$

The classical limit of the approximate FFCF in eq 39 coincides with the exact classical FFCF. To see this, note that in the classical limit: (1) $\langle \boldsymbol{Q_0}|e^{-\beta\hat{H}_b}|\boldsymbol{Q_0}\rangle/Z_b \rightarrow e^{-V(\mathbf{Q}_0)}/\int d\boldsymbol{Q_0}e^{-V(\mathbf{Q}_0)}$; (2) $\alpha^{(j)} \rightarrow 2/\beta\hbar^2$ since $\beta\hbar\Omega^{(j)} \ll 1$, such that $\sum_{j=1}^{N}(P_{n,0}^{(j)})^2/\hbar^2\alpha^{(j)} \rightarrow \beta\sum_{j=1}^{N}(P_{n,0}^{(j)})^2/2 \rightarrow \beta\sum_{j=1}^{N}(P_0{}^{(j)})^2/2M^{(j)}$; (3) $D_T(\boldsymbol{Q_0},\boldsymbol{P_{n,0}})$ and $D_U(\boldsymbol{Q_0},\boldsymbol{P_{n,0}})$, eqs 33 and 36, respectively, vanish as $\hbar \rightarrow 0$, and one is left with averaging over the time correlation of the classical forces, $[\delta F_U(\boldsymbol{Q_0}) + \delta F_T(\boldsymbol{P_0})][\delta F_U(\boldsymbol{Q_t^{(Cl)}}) + \delta F_T(\boldsymbol{P_t^{(Cl)}})]$. It is also important to note that the approximate FFCF satisfies the fundamental quantum-mechanical identity $C(-t) = C^*(t)$, since its the real and imaginary parts are even and odd functions of $\boldsymbol{P_{n,0}}$, respectively (cf. paper I for a more detailed discussion of this point). Finally, we note that whereas the F_U-F_U term in eq 39 is exact at $t = 0$, as shown in paper I, this is not the case for the F_T-F_T and F_U-F_T terms within the current implementation of the LHA. Nevertheless, it should be noted that as long as the LHA is valid, the values of the F_T-F_T and F_U-F_T terms at $t = 0$ are expected to provide a reasonable approximation for the exact quantum result.

IV. Simulation Techniques

The present section discusses the techniques employed for numerically computing $C(t)$ via eq 39. The first step of the simulation involves sampling of the initial positions, $\boldsymbol{Q_0}$. The latter is based on the probability density given by $\langle \boldsymbol{Q_0}|\ e^{-\beta\hat{H}_b}|\boldsymbol{Q_0}\rangle/Z_b$, and can be performed via a PIMD or a PIMC simulation. Discretization of the imaginary-time path using Cartesian coordinates is not trivial in the case of rotational motion, due to the fact that the "on-the-sphere" and "near-the-surface-of-the-sphere" treatments are generally not equivalent.[117] However, those treatments turn out to be equivalent in the case of a linear rotor in 3D (cf. Chapter 8 of ref 117). The rotor's rigidity can be imposed as in standard classical MD simulations,[118] by keeping the distance between the jth beads in the isomorphic cyclic polymer chains that represent the α and β sites of the same molecule fixed throughout the PIMD or PIMC simulation.

A key step in computing the approximate FFCF, eq 39, involves the calculation of the normal-mode frequencies and coordinates that underlie the LHA. It is important to note that the normal mode displacements should be consistent with the fixed bond length constraint. A convenient way for accomplishing this is by actually releasing the constraint at first and then calculating the local normal modes in a system that consists of *flexible* diatomic molecules. More specifically, we introduce an explicit intramolecular harmonic potential that allows the oxygen molecules to vibrate. A sufficiently large vibrational frequency would then give rise to normal-mode frequencies which are much higher than, and well separated from, the frequencies of the rest of the normal modes. The coordinates of these high frequency normal modes correspond to displacements along the internuclear axes. They violate the fixed bond length constraint and are therefore discarded. The remaining normal modes, which correspond to displacements that satisfy the constraint, are kept. It should be emphasized that the molecules are allowed to vibrate only for the sake of finding the normal modes, which is necessary for sampling the initial momenta. Once the latter are obtained, the rigidity constraint is reimposed throughout the subsequent, purely classical, time evolution.

The major computational bottleneck is associated with the high cost of repeatedly calculating the normal-mode frequencies and coordinates of a system with thousands of DOF. However, the effective number of DOF can be drastically reduced if one takes advantage of the fact that the high-frequency FT of the FFCF is dominated by the interaction of the relaxing molecule with the molecules in its first few solvation shells.[119,120] Thus, after sampling the initial positions via a PIMD or PIMC simulation of the overall system (typically consisting of hundreds of molecules in the simulation cell), we randomly select one molecule to be the tagged molecule, and compute the FFCF within a "cluster" that consists of the tagged molecule and a relatively small subset of the molecules closest to it. While the molecules inside the cluster are allowed to move in order to calculate the FFCF, the rest of the molecules are kept frozen at their initial positions and form a static cage that prevents the cluster from falling apart. This procedure is repeated for each sampled initial configuration of the overall system, and the actual prediction for the FFCF consists of an average over many different initial cluster-cage configurations.

A schematic view of the cluster-in-a-liquid (CIL) strategy described above is shown in Figure 1. The following technical points should be noted with regard to it.

•The oxygen molecules in the cluster are not equivalent. Hence, one cannot enhance the efficiency of the computation by considering all of the molecules as tagged, which is a common practice when computing the FFCF in neat liquids via classical MD simulations. However, this loss in computational efficiency is compensated for by the reduced number of effective DOF as well as by the fact that the true computational bottleneck is associated with finding the normal modes.

• The FFCF involves the fluctuations of the instantaneous force relative to its average value, $\delta F = F - \langle F\rangle_0$. $\langle F\rangle_0$ is usually obtained by averaging over time, which is identical to the ensemble average. However, in our case, the force consists of two contributions: one from the dynamical cluster molecules and the other from the static cage molecules. Time-averaging of the force exerted by the frozen cage molecules is obviously impossible. Time-averaging of the force exerted by the cluster

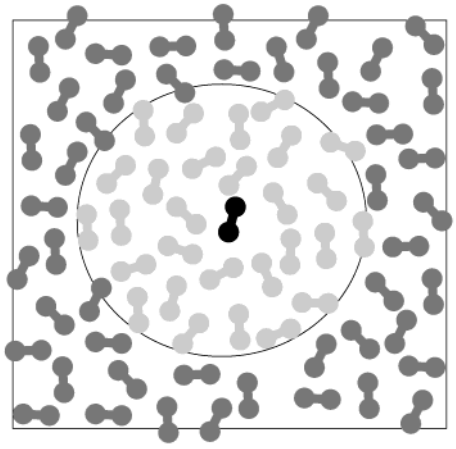

Figure 1. Schematic view of the cluster-in-a-liquid strategy. The tagged molecule (black) is in the center of a cluster which consists of the molecules in its near vicinity (light gray). The molecules that belong to the cluster are "active", in the sense that they are allowed to move, and the LHA−LSC−IVR analysis is performed on them. The rest of the molecules that surround the cluster (dark gray) are frozen and form a static cage that prevents the cluster from falling apart.

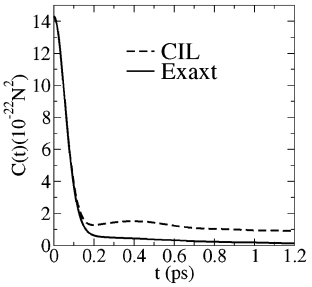

Figure 2. Exact (solid line) and CIL-based (dashed line) FFCFs, as obtained from classical MD simulations of liquid oxygen at a temperature and density of 77 K and 22.64 nm^{-3}, respectively.

molecules is possible, but is generally *different* from the cage-free time-average, which coincide with the ensemble average. We choose to define $\langle F \rangle_0$ as corresponding to the ensemble average, which is the same as the cage-free time average. It should be noted that this procedure ensures that the initial value of the FFCF is identical to that in the cage-free case, but also implies that the computed FFCF does not decay to zero. However, the fact that the FFCF does not decay to zero does not affect its high-frequency FT and our predictions for the VER rate constant.

The validity of the CIL strategy has been tested within the context of a *classical* MD simulation of liquid O_2. In Figure 2, we compare the exact classical FFCF, obtained from a classical MD simulation of 500 oxygen molecules in a simulation cell with periodic boundary conditions (solid line), with the prediction obtained for a cluster consisting of the tagged molecule and 29 of its nearest neighbors, which is surrounded by a cage consisting of additional 60 molecules (dashed line). As expected, the CIL-based FFCF coincides with the exact FFCF at short times, and is different from it at longer times. However, the good agreement at short times suggests that the CIL-based FFCF will capture the high-frequency components of its FT rather well. This is verified in Figure 3, where the FTs of the exact and CIL-based FFCFs are shown on a semilog plot. The main observation is that the high-frequency FT of the CIL-based FFCF coincides with that of the exact FFCF. As is well-known, a reliable evaluation of the extremely small FT of the FFCF at the vibrational frequency of oxygen (1552.5 cm^{-1}) is not feasible

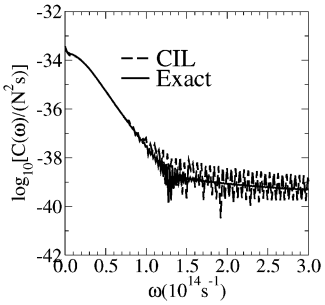

Figure 3. FTs of the exact (solid line) and CIL-based (dashed line) FFCFs, given in terms of a semilog plot, as obtained from classical MD simulations of liquid oxygen, at a temperature and density of 77 K and 22.64 nm^{-3}, respectively.

in practice, due to numerical noise. In the case of Figure 3, a reliable evaluation of the FT of the FFCF has been possible up to a frequency of about 550 cm^{-1}. However, the exponential gap law phenomenology established at these lower frequencies can be assumed to persist to much higher frequencies, such that the value of the FT at the vibrational frequency of oxygen can be obtained by linear extrapolation.[40,41]

It should be noted that the CIL strategy is similar in spirit to, and was in fact inspired by, the instantaneous-pair approach to VER, which was recently introduced by Stratt and co-workers.[119,120] The latter was developed in the context of classical mechanics, and is based on the assumption that high-frequency VER is mediated by the motion of a *single*, instantaneously nearby, solvent molecule. This approach seems to suggest that the computational cost may be further reduced by employing a smaller cluster and more selective initial sampling. However, in light of the already manageable cost of the CIL scheme as described above, no attempt has been made in the current study to further optimize the computational efficiency. Nevertheless, it is likely that such an optimization will be useful when the methodology is applied to more complex systems.

The above discussion suggests the following algorithm for calculating the (approximate) quantum-mechanical FFCF, eq 39, in the case of neat liquid oxygen:

1. Sample $\boldsymbol{Q_0}$ with the probability density $\mathrm{Prob}(\boldsymbol{Q_0}) = \langle \boldsymbol{Q_0}|e^{-\beta \hat{H}_b}|\boldsymbol{Q_0}\rangle/Z_b$ via a PIMD or a PIMC simulation. For the results reported below, a PIMD simulation of 500 O_2 molecules in a cubical simulation cell with periodic boundary conditions, at the temperature of 77 K and density of 22.64 nm^{-3} has been used. Each oxygen atom has been represented by a chain polymer consisting of 16 beads. Thermalization was imposed by attaching a Nose−Hoover chain thermostat to each of the beads, and the dynamics has been computed by using the velocity Verlet algorithm.[121] The sampling was performed by choosing random beads from snapshots of the isomorphic liquid of cyclic polymers.

2. Randomly select one of the 500 molecules and designate it as the tagged molecule. Find the 29 molecules which are closest to the tagged molecule and will form the cluster. Find the next 60 closest molecules that will constitute the static cage which prevents the cluster from falling apart.

3. Apply the LHA to the cluster of 30 "active" molecules, and find the normal-mode frequencies, $\{\Omega^{(k)}\}$, and transformation matrix, $\{T_{k,l}\}$. Use these in order to sample the initial normal mode momenta. It should be noted that the normal-mode analysis and momenta sampling is performed for the cluster molecules only, and therefore involve only 180 DOF. For the results reported below, the Jacobi method has been used for diagonalizing the Hessian matrix.[122]

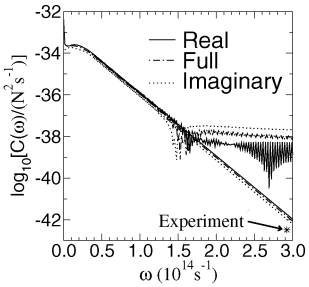

Figure 4. Semilog plot of the FTs of the FFCF, as obtained from the real part of (solid line), imaginary part of (dotted line), and full set of (dashed−dotted) LHA−LSC−IVR-based FFCF. The calculations leading to these results employed the CIL strategy. Simulations were performed on liquid oxygen, at a temperature and density of 77 K and 22.64 nm^{-3}, respectively. Also shown are the experimentally determined value of the FT at the vibrational frequency of oxygen (star), and linear extrapolations of the computed FTs to this frequency.

4. Calculate $\boldsymbol{Q}_t^{(Cl)}$ and $\boldsymbol{P}_t^{(Cl)}$ for the cluster molecules via a classical MD simulation, and time correlate $\delta F(\boldsymbol{Q}_t^{(Cl)},\boldsymbol{Q}_t^{(Cl)})$ with $\delta F(\boldsymbol{Q_0},\boldsymbol{P_0})$, $D_U(\boldsymbol{Q_0},\boldsymbol{P}_{n,0})$ and $D_T(\boldsymbol{Q_0},\boldsymbol{P}_{n,0})$ (corresponding to the force on the tagged molecule). The velocity Verlet algorithm with a time step of 4 fs has been used in the simulations reported here.

5. Repeat steps 1−4 for many initial cluster−cage configurations, and average the results in order to obtain the desired FFCF.

V. Results

In this section, we present results that were obtained by using the semiclassical methodology outlined above for calculating the FFCF in the case of neat liquid oxygen. All of the results were obtained with the model potential described above, at a temperature of 77 K and density of 22.64 nm^{-3}. We note that a classical calculation of the VER rate constant for neat liquid oxygen under the same conditions has been recently reported by Everitt et al.[59]

In Figure 4, we show, on a semilog plot, the FT of the LHA−LSC−IVR FFCF, as obtained from either the full FFCF, its real part or its imaginary part [for the exact FFCF, $\tilde{C}(\omega) = 4\int_0^\infty dt\ \cos(\omega t)C_R(t)/(1 + e^{-\beta\hbar\omega}) = -4\int_0^\infty dt\ \sin(\omega t)C_I(t)/(1 - e^{-\beta\hbar\omega})$; cf. eq 18]. As for the other model systems previously considered, the difference between the predictions is found to be rather small. Linear extrapolation to the frequency of oxygen reveals that the best agreement with experiment is obtained when the imaginary part is used. However, we believe that this observation is incidental and that the FT obtained from the real part actually provides the least approximate estimate (cf. paper I for a more detailed discussion of this point). We would therefore restrict ourselves to the FT obtained from the real part in what follows.

In Figure 5, we compare the real part of the LHA−LSC−IVR FFCF with the corresponding classical result. The initial values of the LHA−LSC−IVR FFCF is seen to be significantly larger than the corresponding classical prediction. This is consistent with a similar observation made in paper I in the case of a LJ breathing sphere model. The larger quantum-mechanical force amplitude is a manifestation of the important role played by delocalization. The effect of the latter is probably enhanced in the FFCF due to the high sensitivity of the force to displacements at the region of the repulsive wall.

In Figure 6, we compare the FT of the LHA−LSC−IVR FFCF with the predictions obtained by using various QCFs. The actual values of the FTs at the frequency of oxygen were obtained by linear extrapolation, as discussed above. The

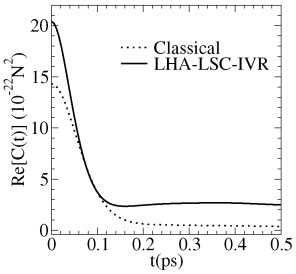

Figure 5. Real part of the FFCF as obtained from LHA−LSC−IVR, within the CIL approximation (solid line). Also shown is the fully classical FFCF (dotted line). The calculations were performed on liquid oxygen, at a temperature and density of 77 K and 22.64 nm^{-3}, respectively.

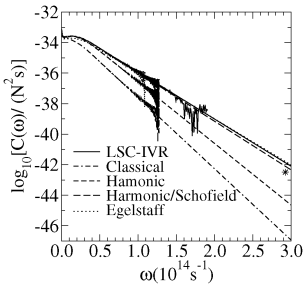

Figure 6. Semilog plot of the FT of the FFCF as obtained from LHA−LSC−IVR (solid line), fully classical (dashed−dotted line), the harmonic QCF (short dashed line), the mixed harmonic-Schofield QCF (long dashed line), and Egelstaff QCF (dotted line). The results apply to liquid oxygen, at a temperature and density of 77 K and 22.64 nm^{-3}, respectively. Also shown are the experimentally determined value of the FT at the vibrational frequency of oxygen (star), and linear extrapolations of the computed FTs to this frequency.

corresponding values of $k_{0\leftarrow1}$ are given in Table 1. The LHA−LSC−IVR result is larger than the experimental result by a factor of 4. This should be compared to the much larger gap of 4 orders of magnitude that separates the experimental result from the classical prediction (cf. Table 1). We therefore consider the LHA−LSC−IVR prediction as being in very good quantitative agreement with experiment. The level of agreement is also comparable to that obtained via the best performing QCF (the mixed harmonic−Schofield QCF). It should be emphasized however that it is usually difficult to predict which, if any, QCF will perform the best for a given system. This should be contrasted with the LHA−LSC−IVR method presented herein, where the quantum correction automatically adapts itself to the system under study, and does not require any guess work. It should also be noted that the residual deviation from the experimental value may well be due to experimental errors and/or inaccuracies in the potentials, whose development has been largely based on fitting to bulk thermodynamic data.

The relative contributions of the potential and centrifugal forces to the LSC−IVR FFCF are shown in Figure 7. Only the diagonal F_U-F_U and F_T-F_T terms are shown (the F_T-F_U and F_U-F_T cross terms are not explicitly shown and can be inferred from the difference between the full FFCF and the sum of the diagonal terms). As for the classical case, one finds that the potential force is more dominant, although the contribution of the centrifugal force is certainly not negligible. In fact the relative weight of both terms is comparable to the classical case, and both are seen to be enhanced by quantum effects in a similar manner. The contributions of these diagonal terms to the FT of the FFCF are shown in Figure 8. Although the contribution of the potential force remain larger than that of the centrifugal force as the frequency increases, which is consistent with the classical

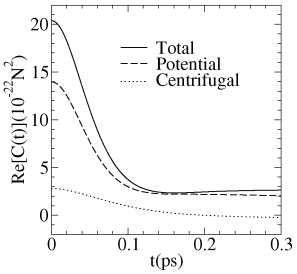

Figure 7. Relative contributions of the potential and centrifugal forces to the real part of the LHA−LSC−IVR FFCF, within the CIL approximation. The cross term is not explicitly shown and can be inferred from the difference between the total FFCF and the diagonal contributions. The results apply to liquid oxygen, at a temperature and density of 77 K and 22.64 nm^{-3}, respectively.

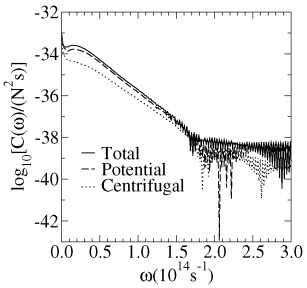

Figure 8. Relative contributions of the potential and centrifugal forces to the FT of the FFCF as calculated from LHA−LSC−IVR, within the CIL approximation. The results apply to liquid oxygen, at a temperature and density of 77 K and 22.64 nm^{-3}, respectively.

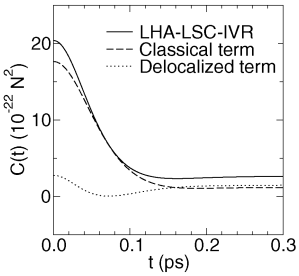

Figure 9. Relative contribution of the classical term, $\delta F(\boldsymbol{Q_0}, \boldsymbol{P_{n,0}})$, and purely quantum-mechanical term, $D(\boldsymbol{Q_0}, \boldsymbol{P_{n,0}})$, to the real part of the LSC− IVR FFCF.

behavior,[43,59] the actual difference between the two contributions diminishes as the frequency increases, which is different from what is observed classically.

The relative contributions of the classical term, $\delta F(\boldsymbol{Q_0},\boldsymbol{P_{n,0}}) = \delta F_T(\boldsymbol{P_{n,0}}) + \delta F_U(\boldsymbol{Q_0})$, and purely quantum mechanical delocalized term, $D(\boldsymbol{Q_0},\boldsymbol{P_{n,0}}) = D_T(\boldsymbol{Q_0},\boldsymbol{P_{n,0}}) + D_U(\boldsymbol{Q_0},\boldsymbol{P_{n,0}})$, to the real part of the LSC−IVR FFCF, eq 39, is shown in Figure 9. As can be seen, the classical term appears to be dominant when the FFCF is presented in the time domain. However, we found that the delocalized term dominates as the focus shifts to the high frequency FT of the FFCF, as can be seen in Figure 10. This observation is consistent with what we have seen in other models (cf. paper I), and suggests that high-frequency VER originates from a purely quantum-mechanical term which is not accounted for in classical MD simulations.

VI. Conclusions

The ability of LSC−IVR to capture quantum effects over a short period of time suggests that it is well suited for estimating relatively short lived quantum-mechanical correlation functions in condensed phase systems. The validity of this hypothesis has

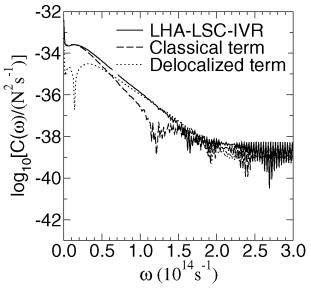

Figure 10. Relative contribution of the classical term, $\delta F(\boldsymbol{Q_0}, \boldsymbol{P_{n,0}})$, and purely quantum-mechanical term, $D(\boldsymbol{Q_0}, \boldsymbol{P_{n,0}})$, to the FT of the LHA−LSC−IVR FFCF. The log of the absolute value of the $D(\boldsymbol{Q_0}, \boldsymbol{P_{n,0}})$ term is plotted since it is negative at small frequencies.

been previously demonstrated in the calculation of reaction rate constants, which depend on the short time dynamics of the flux−flux correlation function.[72,123] VER rate constants can be given in terms of the FT, at the vibrational frequency, of the quantum-mechanical FFCF, and are known to deviate by orders of magnitudes relative to the corresponding classical prediction. In paper I, we proposed and tested an LSC−IVR-based method for calculating the FFCF, and hence VER rate constants in condensed phase systems. In the present paper, we have extended this method to the case of molecular liquids. New features include the incorporation of centrifugal forces, as well as the computational tools necessary for calculating the FFCF in a constrained system with many DOF. The resulting LHA−LSC−IVR method was then applied to the challenging problem of calculating the extremely slow and highly quantum-mechanical VER rate constant in liquid oxygen. The result was found to be in very good agreement with experiment, thereby providing further support for the validity and feasibility of an LSC−IVR-based approach to VER in liquid solutions.

The success of LSC−IVR should probably be attributed to its ability to capture the correct short time behavior of the quantum-mechanical FFCF, which in turn dominates its high-frequency FT and hence the VER rate constant. In this respect, LSC−IVR is ideally suited for the VER problem. The computational framework developed in the present paper also turn LSC−IVR into a feasible method, which can be applied to realistic models of molecular liquids. As such, it provides a very attractive alternative to the common practice of multiplying the classical VER rate constant by a rather ad hoc QCF. Future applications to other molecular liquids, as well as the development of more efficient computational tools are currently underway, and these will be the subject of future publications.

Acknowledgment. The authors are grateful for financial support from the National Science Foundation through Grant No. CHE-0306695.

References and Notes

(1) Oxtoby, D. W. *Adv. Chem. Phys.* **1981**, *47 (Part 2)*, 487.
(2) Oxtoby, D. W. *Annu. Rev. Phys. Chem.* **1981**, *32*, 77.
(3) Oxtoby, D. W. *J. Phys. Chem.* **1983**, *87*, 3028.
(4) Chesnoy, J.; Gale, G. M. *Ann. Phys. Fr.* **1984**, *9*, 893.
(5) Chesnoy, J.; Gale, G. M. *Adv. Chem. Phys.* **1988**, *70 (Part 2)*, 297.
(6) Harris, C. B.; Smith, D. E.; Russell, D. J. *Chem. Rev.* **1990**, *90*, 481.
(7) Miller, D. W.; Adelman, S. A. *Int. Rev. Phys. Chem.* **1994**, *13*, 359.
(8) Stratt, R. M.; Maroncelli, M. *J. Phys. Chem.* **1996**, *100*, 12981.
(9) Owrutsky, J. C.; Raftery, D.; Hochstrasser, R. M. *Annu. Rev. Phys. Chem.* **1994**, *45*, 519.
(10) Elsaesser, T.; Kaiser, W. *Annu. Rev. Phys. Chem.* **1991**, *42*, 83.
(11) Calaway, W. F.; Ewing, G. E. *J. Chem. Phys.* **1975**, *63*, 2842.
(12) Brueck, S. R. J.; Osgood, R. M. *Chem. Phys. Lett.* **1976**, *39*, 568.

(13) Laubereau, A.; Kaiser, W. *Rev. Mod. Phys.* **1978**, *50*, 607.
(14) Faltermeier, B.; Protz, R.; Maier, M.; Werner, E. *Chem. Phys. Lett.* **1980**, *74*, 425.
(15) Faltermeier, B.; Protz, R.; Maier, M. *Chem. Phys.* **1981**, *62*, 377.
(16) Chateau, M.; Delalande, C.; Frey, R.; Gale, G. M.; Pradère, F. *J. Chem. Phys.* **1979**, *71*, 4799.
(17) Delalande, C.; Gale, G. M. *J. Chem. Phys.* **1980**, *73*, 1918.
(18) Roussignol, P.; Delalande, C.; Gale, G. M. *Chem. Phys.* **1982**, *70*, 319.
(19) Heilweil, E. J.; Doany, F. E.; Moore, R.; Hochstrasser, R. M. *J. Chem. Phys.* **1982**, *76*, 5632.
(20) Heilweil, E. J.; Casassa, M. P.; Cavanagh, R. R.; Stephenson, J. C. *Chem. Phys. Lett.* **1985**, *117*, 185.
(21) Heilweil, E. J.; Casassa, M. P.; Cavanagh, R. R.; Stephenson, J. C. *J. Chem. Phys.* **1986**, *85*, 5004.
(22) Harris, A. L.; Brown, J. K.; Harris, C. B. *Annu. Rev. Phys. Chem* **1988**, *39*, 341.
(23) Paige, M. E.; Russell, D. J.; Harris, C. B. *J. Chem. Phys.* **1986**, *85*, 3699.
(24) Owrutsky, J. C.; Kim, Y. R.; Li, M.; Sarisky, M. J.; Hochstrasser, R. M. *Chem. Phys. Lett.* **1991**, *184*, 368.
(25) Moustakas, A.; Weitz, E. *J. Chem. Phys.* **1993**, *98*, 6947.
(26) Kliner, D. A. V.; Alfano, J. C.; Barbara, P. F. *J. Chem. Phys.* **1993**, *98*, 5375.
(27) Zimdars, D.; Tokmakoff, A.; Chen, S.; Greenfield, S. R.; Fayer, M. D. *Phys. Rev. Lett.* **1993**, *70*, 2718.
(28) Pugliano, N.; Szarka, A. Z.; Gnanakaran, S.; Hochstrasser, R. M. *J. Chem. Phys.* **1995**, *103*, 6498.
(29) Paige, M. E.; Harris, C. B. *Chem. Phys.* **1990**, *149*, 37.
(30) Salloum, A.; Dubost, H. *Chem. Phys.* **1994**, *189*, 179.
(31) Tokmakoff, A.; Sauter, B.; Fayer, M. D. *J. Chem. Phys.* **1994**, *100*, 9035.
(32) Tokmakoff, A.; Fayer, M. D. *J. Chem. Phys.* **1995**, *103*, 2810.
(33) Urdahl, R. S.; Myers, D. J.; Rector, K. D.; Davis, P. H.; Cherayil, B. J.; Fayer, M. D. *J. Chem. Phys.* **1997**, *107*, 3747.
(34) Owrutsky, J. C.; Li, M.; Locke, B.; Hochstrasser, R. M. *J. Phys. Chem.* **1995**, *99*, 4842.
(35) Laenen, R.; Rauscher, C.; Laubereau, A. *Phys. Rev. Lett.* **1998**, *80*, 2622.
(36) Woutersen, S.; Emmerichs, U.; Nienhuys, H.; Bakker, H. J. *Phys. Rev. Lett.* **1998**, *81*, 1106.
(37) Myers, D. J.; Chen, S.; Shigeiwa, M.; Cherayil, B. J.; Fayer, M. D. *J. Chem. Phys.* **1998**, *109*, 5971.
(38) Sagnella, D. E.; Straub, J. E.; Jackson, T. A.; Lim, M.; Anfinrud, P. A. *Proc. Natl. Acad. Sci. U.S.A.* **1999**, *96*, 14324.
(39) Hamm, P.; Lim, M.; Hochstrasser, R. M. *J. Chem. Phys.* **1997**, *107*, 1523.
(40) Nitzan, A.; Mukamel, S.; Jortner, J. *J. Chem. Phys.* **1974**, *60*, 3929.
(41) Nitzan, A.; Mukamel, S.; Jortner, J. *J. Chem. Phys.* **1975**, *63*, 200.
(42) Egorov, S. A.; Skinner, J. L. *J. Chem. Phys.* **1996**, *105*, 7047.
(43) Everitt, K. F.; Egorov, S. A.; Skinner, J. L. *Chem. Phys.* **1998**, *235*, 115.
(44) Everitt, K. F.; Skinner, J. L. *J. Chem. Phys.* **1999**, *110*, 4467.
(45) Poulsen, J.; Rossky, P. J. *J. Chem. Phys.* **2001**, *115*, 8014.
(46) Douglass, D. C. *J. Chem. Phys.* **1961**, *35*, 81.
(47) Adelman, S. A.; Stote, R. H. *J. Chem. Phys.* **1988**, *88*, 4397.
(48) Stote, R. H.; Adelman, S. A. *J. Chem. Phys.* **1988**, *88*, 4415.
(49) Adelman, S. A.; Muralidhar, R.; Stote, R. H. *J. Chem. Phys.* **1991**, *95*, 2738.
(50) Rabani, E.; Reichman, D. R. *J. Phys. Chem. B* **2001**, *105*, 6550.
(51) Makri, N. *Annu. Rev. Phys. Chem.* **1999**, *50*, 167.
(52) Berne, B. J.; Jortner, J.; Gordon, R. *J. Chem. Phys.* **1967**, *47*, 1600.
(53) Bader, J. S.; Berne, B. J. *J. Chem. Phys.* **1994**, *100*, 8359.
(54) Egorov, S. A.; Everitt, K. F.; Skinner, J. L. *J. Phys. Chem. A* **1999**, *103*, 9494.
(55) Egorov, S. A.; Skinner, J. L. *J. Chem. Phys.* **2000**, *112*, 275.
(56) Skinner, J. L.; Park, K. *J. Phys. Chem. B* **2001**, *105*, 6716.
(57) Rostkier-Edelstein, D.; Graf, P.; Nitzan, A. *J. Chem. Phys.* **1997**, *107*, 10470.
(58) Rostkier-Edelstein, D.; Graf, P.; Nitzan, A. *J. Chem. Phys.* **1998**, *108*, 9598.
(59) Everitt, K. F.; Skinner, J. L.; Ladanyi, B. M. *J. Chem. Phys.* **2002**, *116*, 179.
(60) Berens, P. H.; White, S. R.; Wilson, K. R. *J. Chem. Phys.* **1981**, *75*, 515.
(61) Frommhold, L. Collision-induced absorption in gases. In *Cambridge Monographs on Atomic, Molecular, and Chemical Physics*, 1st ed.; Cambridge University Press: Cambridge, England, 1993; Vol 2.
(62) Skinner, J. L. *J. Chem. Phys.* **1997**, *107*, 8717.
(63) An, S. C.; Montrose, C. J.; Litovitz, T. A. *J. Chem. Phys.* **1976**, *64*, 3717.
(64) Egorov, S. A.; Skinner, J. L. *Chem. Phys. Lett.* **1998**, *293*, 439.
(65) Schofield, P. *Phys. Rev. Lett.* **1960**, *4*, 239.
(66) Egelstaff, P. A. *Adv. Phys.* **1962**, *11*, 203.
(67) Kneller, G. R. *Mol. Phys.* **1994**, *83*, 63.
(68) Sun, X.; Miller, W. H. *J. Chem. Phys.* **1997**, *106*, 916.
(69) Wang, H.; Sun, X.; Miller, W. H. *J. Chem. Phys.* **1998**, *108*, 9726.
(70) Sun, X.; Wang, H.; Miller, W. H. *J. Chem. Phys.* **1998**, *109*, 4190.
(71) Sun, X.; Wang, H.; Miller, W. H. *J. Chem. Phys.* **1998**, *109*, 7064.
(72) Wang, H.; Song, X.; Chandler, D.; Miller, W. H. *J. Chem. Phys.* **1999**, *110*, 4828.
(73) Sun, X.; Miller, W. H. *J. Chem. Phys.* **1999**, *110*, 6635.
(74) Wang, H.; Thoss, M.; Miller, W. H. *J. Chem. Phys.* **2000**, *112*, 47.
(75) Vleck, J. H. V. *Proc. Nat. Acad. Sci.* **1928**, *14*, 178.
(76) Gutzwiller, M. C. *J. Math. Phys.* **1967**, *8*, 1979.
(77) Gutzwiller, M. C. *J. Math. Phys.* **1971**, *12*, 343.
(78) Gutzwiller, M. C. *Chaos in Classical and Quantum Mechanics*; Springer-Verlag: Berlin, 1990.
(79) Littlejohn, R. G. *J. Stat. Phys.* **1992**, *68*, 7.
(80) Pechukas, P. *Phys. Rev.* **1969**, *181*, 174.
(81) Levit, S.; Smilansky, U. *Ann. Phys. (N.Y.)* **1977**, *108*, 165.
(82) Levit, S.; Mohring, K.; Smilansky, U.; Dreyfus, T. *Ann. Phys. (N.Y.)* **1978**, *114*, 223.
(83) Maslov, V. P.; Fedoriouk, M. V. *Semiclassical approximation in quantum mechanics*; Reidel: Boston, MA, 1981.
(84) Pollak, E.; Liao, J. *J. Chem. Phys.* **1998**, *108*, 2733.
(85) Miller, W. H. *Adv. Chem. Phys.* **1974**, *25*, 69.
(86) Miller, W. H. *J. Chem. Phys.* **1970**, *53*, 3578.
(87) Herman, M. F.; Kluk, E. *Chem. Phys.* **1984**, *91*, 27.
(88) Heller, E. J. *J. Chem. Phys.* **1981**, *94*, 2723.
(89) Kay, K. G. *J. Chem. Phys.* **1994**, *100*, 4377.
(90) Ovchinnikov, M.; Apkarian, V. A. *J. Chem. Phys.* **1996**, *105*, 10312.
(91) Ovchinnikov, M.; Apkarian, V. A. *J. Chem. Phys.* **1998**, *108*, 2277.
(92) Makri, N.; Thompson, K. *Chem. Phys. Lett.* **1998**, *291*, 101.
(93) Miller, W. H. *Faraday, Discuss.* **1998**, *110*, 1.
(94) Shao, J. S.; Makri, N. *J. Phys. Chem. A* **1999**, *103*, 7753.
(95) Thompson, K.; Makri, N. *Phys. Rev. E* **1999**, *59*, R4729.
(96) Kühn, O.; Makri, N. *J. Phys. Chem. A* **1999**, *103*, 9487.
(97) Ovchinnikov, M.; Apkarian, V. A.; Voth, G. A. *J. Chem. Phys.* **2001**, *184*, 7130.
(98) Miller, W. H. *J. Phys. Chem. A* **2001**, *105*, 2942.
(99) Makri, N.; Miller, W. H. *J. Chem. Phys.* **2002**, *116*, 9207.
(100) Miller, W. H. *J. Chem. Phys.* **1991**, *95*, 9428.
(101) Heller, E. J. *J. Chem. Phys.* **1991**, *95*, 9431.
(102) Kluk, E.; Herman, M. F.; Davis, H. L. *J. Chem. Phys.* **1986**, *84*, 326.
(103) Kay, K. G. *J. Chem. Phys.* **1994**, *101*, 2250.
(104) Provost, D.; Brumer, P. *Phys. Rev. Lett.* **1995**, *74*, 250.
(105) Garashchuk, S.; Tannor, D. *Chem. Phys. Lett.* **1996**, *262*, 477.
(106) Keshavamurthy, S.; Miller, W. H. *Chem. Phys. Lett.* **1994**, *218*, 183.
(107) Spath, B. W.; Miller, W. H. *J. Chem. Phys.* **1996**, *104*, 95.
(108) Shi, Q.; Geva, E. *J. Chem. Phys.* **2003**, *118*, 8173.
(109) Hillery, M.; O'Connell, R. F.; Scully, M. O.; Wigner, E. P. *Phys. Rep.* **1984**, *106* (3), 121.
(110) Perng, B.; Sasaki, S.; Ladanyi, B. M.; Everitt, K. F.; Skinner, J. L. *J. Lumin.* **2001**, *348*, 491.
(111) Berne, B. J.; Gordon, R. G.; Sears, V. F. *J. Chem. Phys.* **1968**, *49*, 475.
(112) Rey, R.; Hynes, J. T. *J. Chem. Phys.* **1996**, *104*, 2356.
(113) Whitnell, R. M.; Wilson, K. R.; Hynes, J. T. *J. Phys. Chem.* **1990**, *94*, 8625.
(114) Gai, H.; Voth, G. A. *J. Chem. Phys.* **1993**, *99*, 740.
(115) Gnanakaran, S.; Hochstrasser, R. M. *J. Chem. Phys.* **1996**, *105*, 3486.
(116) Zwanzig, R. *J. Chem. Phys.* **1961**, *34*, 1931.
(117) Kleinert, H. *Path integrals in quantum mechanics, statistics and polymer physics*; World Scientific: River Edge, NJ, 1995.
(118) Allen, M. P.; Tildesley, D. J. *Computer Simulation of Liquids*; Clarendon: Oxford, England, 1987.
(119) Larsen, R.; Stratt, R. M. *J. Chem. Phys.* **1999**, *110*, 1036.
(120) Deng, Y.; Stratt, R. M. *J. Chem. Phys.* **2002**, *117*, 10752.
(121) Jang, S.; Voth, G. A. *J. Chem. Phys.* **1997**, *107*, 9514.
(122) Press, W. H.; Flannery, B. P.; Teukolsky, S. A.; Vetterling, W. T. *Numerical Recipes*; Cambridge University Press: Cambridge, England, 1986.
(123) Liao, J. L.; Pollak, E. *J. Chem. Phys.* **2002**, *116*, 2718.
(124) Shi, Q; Geva, E. *J. Phys. Chem. A* **2003**, *107*, 9059.